# Characterization of a resistive ribbon thermal transfer printing process

by T. G. Twardeck

Resistive ribbon thermal transfer printers transfer ink from a ribbon to paper as the result of localized Joule heating of the ribbon structure. For this printing process, this paper discusses the voltage-versus-current response of the electrode-ribbon current path, the temperature distributions throughout the ribbon structure, and the correlation of print response with electrical input power and average ribbon temperatures. Nominal input power per electrode is approximately 190 mW. For input power near this level, thermal models predict that ribbon materials which pass directly under energized electrodes reach the highest temperatures; the hottest zone in the ribbon surrounds the composite-aluminum interface. Approximately 0.1 mm downstream from the electrodes, the heated ribbon materials come to nearly constant temperature. The area of the printed image correlates with this average ribbon temperature and input power.

### Introduction

Conventional thermal transfer printers transfer ink from a ribbon to paper as the result of localized heating of the

**Copyright** 1985 by International Business Machines Corporation. Copying in printed form for private use is permitted without payment of royalty provided that (1) each reproduction is done without alteration and (2) the *Journal* reference and IBM copyright notice are included on the first page. The title and abstract, but no other portions, of this paper may be copied or distributed royalty free without further permission by computer-based and other information-service systems. Permission to *republish* any other portion of this paper must be obtained from the Editor.

ribbon structure. In one typical arrangement of this printing process, an array of heating elements forces the ribbon against the paper. The ribbon during printing is stationary with respect to the paper, while the heating elements make sliding contact with the ribbon. When electrical current flows in a heating element, a significant rise in its temperature occurs. The resultant heat flow into a small volume of the ribbon material melts the ink, transferring it to the paper. Continuous current flow in a moving electrode results in the transfer of a strip of ink to the paper. The strips from many electrodes can be adjusted in length and spatial arrangement to form characters.

An alternate means of achieving thermal ink transfer with this general printing scheme incorporates electrically resistive elements into the body of the ribbon [1–3]. Electrodes in this situation inject current into the ribbon. The result of current flow is direct heating of the conductive ribbon materials. The heating is sufficiently intense to soften the ink and transfer it to the paper. One advantage of this latter approach is related to printing speed. Direct heating of the ribbon in combination with highly conductive electrodes reduces the print speed restrictions that are inherent with conventional thermal transfer printers. Further, new printhead structures and transfer layer materials yield excellent print quality on a wide range of plain office papers.

This paper considers some of the electrical, thermal, and imaging aspects of this thermal printing technique, which uses electrical current flow through the ribbon structure to produce the heat for printing. The information provided for the process, which is called resistive ribbon thermal transfer printing, illustrates some of the key characteristics of this novel printing process. Both the \*QUIETWRITER Printer and

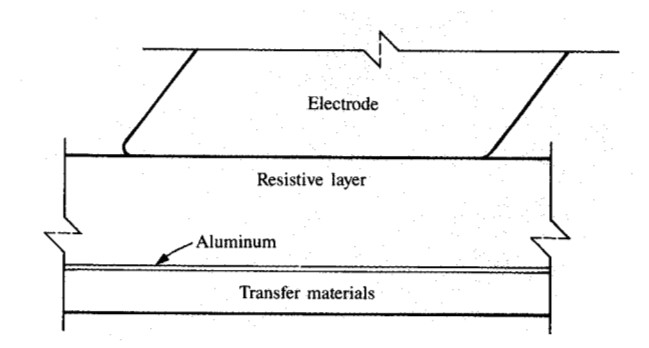
QUIETWRITER Typewriter print characters with such a process. The specific application of the printing process in these products is discussed in this paper.

Figure 1 shows a cross section of the electrode and multilayered ribbon. For the printer and typewriter, the printhead electrodes are etched from tungsten foil and have contact tips arranged along a common axis on 0.11-mm (0.00417-in.) center-to-center spacings. Contact surfaces are subsequently finished to dimensions of approximately 0.05 mm  $\times 0.05$  mm (0.002 in.  $\times 0.002$  in.). During printing the electrodes slide at a rate of 102 mm/s (4 in./s) on the surface of the ribbon. Electric current flows into the ribbon via these electrodes and constant current sources. The ribbon layer in contact with the electrodes is a conductive carbon blackpolycarbonate composite. This "resistive layer," approximately 15 µm in thickness, has a bulk electrical resistivity of roughly 0.75  $\Omega$ -cm. A second layer of the ribbon, aluminum, is vapor-deposited on the surface of the resistive layer opposite the electrodes. The thickness of the aluminum layer is approximately 100 nm. These two layers form part of the current flow path in the ribbon. The remaining structure of the ribbon consists of transfer (ink) materials.

In this electrode-ribbon configuration, electrical current flows into the resistive layer and then along the aluminum layer to a ground return path. The heat generated from electrical current flow along this path results in the transfer of a print character to the page. The important elements in the current flow path for the generation of heat in the printing process are considered in detail. These elements include the electrode-resistive layer contact resistance, the bulk of the resistive layer, and the interface region of the resistive and aluminum layers. Experiments illustrating the voltage-current response of these elements are presented. The experimental results are used in a discussion of typical voltage-current characteristics of the electrode-ribbon structure. The temperatures produced in the electrode and ribbon are determined through model simulation. The simulated results are compared with direct temperature measurements. As a measure of process performance, the size of the print character on the paper is discussed.

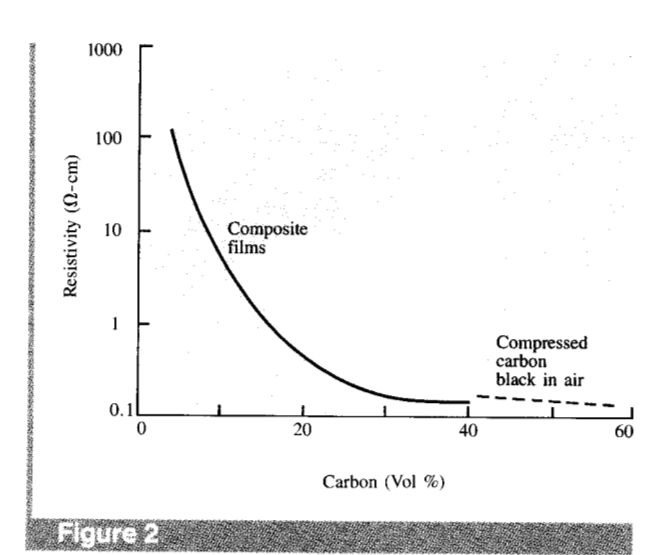
# **Electrical response**

This section begins with a discussion of the polycarbonate-carbon black composite, the resistive layer in the ribbon. The composite is characterized in terms of the bulk electrical resistivity as a function of carbon content and also with respect to the change in its resistivity as a function of temperature for a given carbon content. The two composite-metal junctions formed at the composite-aluminum (stationary) interface and the composite-tungsten (sliding) interface are considered. The voltage-current responses of these regions and those of the electrode-ribbon structure are discussed.



### Feller

Enlarged sectional view of the electrode and ribbon for resistive ribbon thermal transfer printing process.



Electrical resistivity versus volume percent of carbon black loading for carbon-polycarbonate composite films (solid line); resistivity versus volume percent of compressed carbon black in air (broken line).

The two components in the resistive layer of the ribbon are polycarbonate, chosen for thermal stability and tensile properties, and a carbon black selected for relatively high electrical conductivity. A mixture of these two components is solvent-cast to form a film nominally 15  $\mu$ m in thickness. Figure 2 shows typical resistivities of such films for carbon contents varying between 5 and 40 volume percent (6 to 50 weight percent). The plotted resistivity values are the results of four probe dc voltage-current measurements at nominal room environments. The solid line in the figure relates to films made as laboratory samples. The broken line refers to measurements of compressed carbon black in air. Note for reference purposes that the resistivity of an unfilled

the polymer. Between these two extremes, a threshold in resistivity occurs. Athough this theory agrees with the general shape of Fig. 2 and the low-temperature region of Fig. 3, more quantitative estimates are not available because the geometric constants of the carbon-polymer configuration are difficult to establish.

In the current flow path of the printing process, the composite behaves as a temperature-dependent resistive element. To illustrate the form of the voltage-current response of this region, consider a sheet of the composite material coated with a layer of gold on one side and with a small-diameter gold dot applied to the second surface. Suppose that a direct current which ramps up as a function of time is made to flow from the gold dot through the resistive layer into the gold layer. The voltage required to sustain this current density at the gold dot. This linear function of current density at the gold dot. This linear response holds for ramp times that are short enough to prevent composite heating. If the conditions of the test cause tresistive layer heating, the voltages required to sustain the resistive layer heating, the voltages required to sustain the current ramp increase (over those shown) with current current ramp increase (over those shown) with current current

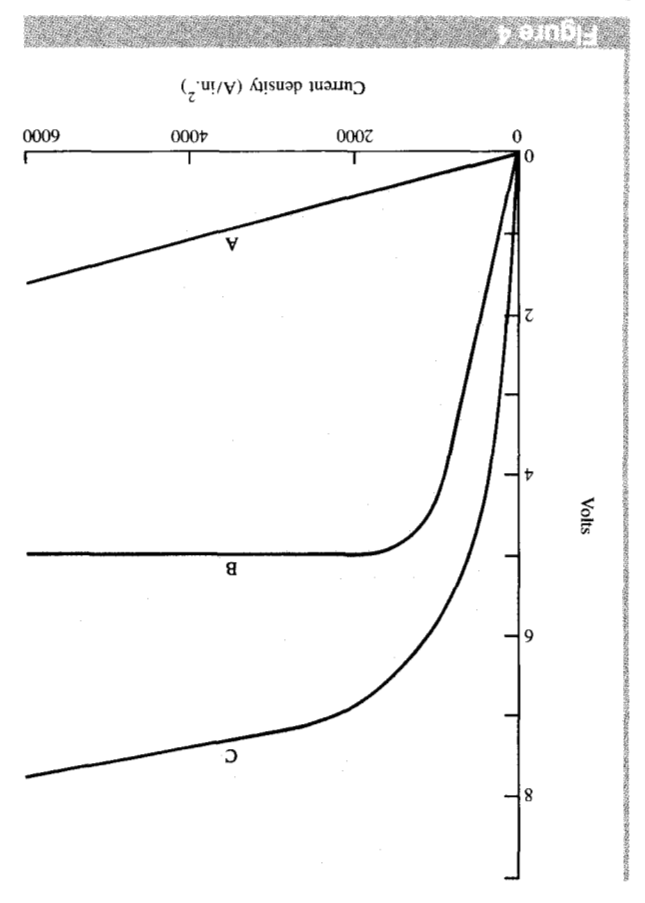
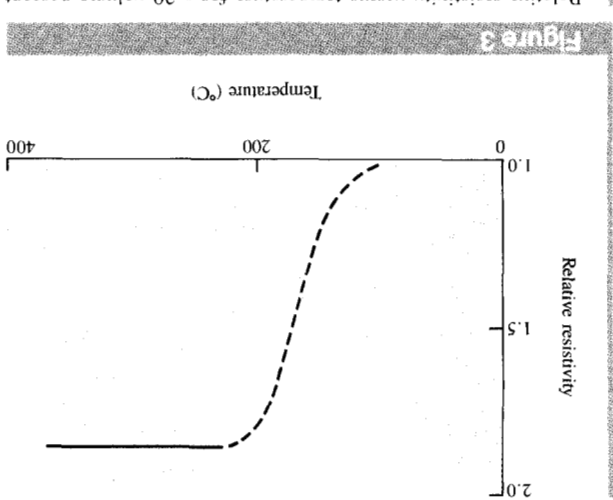


Illustration of voltage versus current density: Curve A, gold dotresistive layer-gold; Curve B, resistive layer-aluminum junction; Curve C, metal probe-resistive layer-aluminum.



Relative resistivity versus temperature for a 20 volume percent carbon-polycarbonate film.

polycarbonate is about 10<sup>17</sup>  $\Omega$ -cm. Figure 3 shows the change in relative resistivity with temperature for a film with 20 volume percent of carbon black. The resistivity rises slowly from room temperature to nearly the glass transition temperature of the polymer. Above this temperature and over a small range of higher values the dimensions of the film change rapidly and its resistivity stabilizes at approximately 1.7 times the room-temperature resistivity. An inquiry into the general form of the data in Figs. 2 and An inquiry into the general form of the data in Figs. 2 and

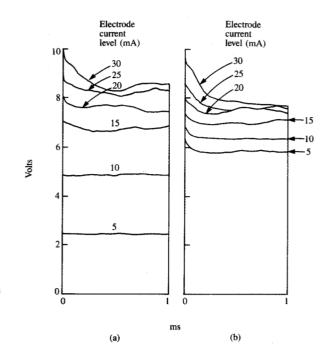
composite resistivity is independent of the filler constituent temperature. For very light conductor loadings, the predicted above ambient and approach the glass transition predicts a slowly increasing resistivity as temperatures rise carbon black. At extreme conductor loading, the theory conducting filler compares favorably with that of compressed composite resistivity at 40 percent volume fraction of validity of this prediction is evident in Fig. 2, where the takes on the electrical properties of the filler material. The composite resistivity is independent of the tunnel gaps and concentrations far above the threshold value, the predicted volume data of the host polymer. For conductor dependent by further incorporating into the model specific The separation between particles can be made temperature account for electron tunneling between conducting particles. combined with quantum-mechanical considerations to On a microscopic basis the percolation formalism is concentration passes through some critical threshold value. a large change in resistivity as the conductor-filler effective medium form of percolation theory to demonstrate filled polymers. From a macroscopic viewpoint, they use the processes that govern electron transport through conductor-Their paper provides a unifying model for the physical 3 can proceed according to the work of Sherman et al. [4].

and is instead dominated by the bulk insulating properties of

density. [Note: The circuit resistance can be estimated for this simple geometry through an application of electrostatic theory, assuming a circular dot, perfect conductivity of the metals, and a resistive layer characterized by a constant resistivity. Calculations compare with measurements to within a few percent. It is concluded that vapor-deposited gold contacts do not appreciably add to the circuit resistance.]

The resistive layer-aluminum interface in the ribbon structure is formed by the vapor deposition of aluminum on the resistive layer. Electrical current flow through this interface is another heat source in the ribbon, and because this region is closest to the transfer layers it makes an important contribution in the thermal transfer of the print character to the paper. The voltage-current response of this region can be obtained by recording the voltage required to sustain a current ramp through a structure consisting of a gold dot-resistive layer-aluminum layer. The voltage in such a test is plotted as a function of current density at the gold dot in curve B of Fig. 4. The voltage in curve B has been corrected for the voltage drop across the resistive layer; that is, the corresponding voltages in curve A have been subtracted from the measured voltages for the gold dotresistive layer-aluminum layer configuration. Curve B indicates that the resistive layer-aluminum junction has a highly nonlinear voltage-current behavior. For low current densities at the injection electrode, this junction has nearohmic behavior, with voltage rising with increasing current. This trend continues until the voltage drop across the junction reaches approximately 5 V. The junction voltage stabilizes at this value and passes the higher current densities at essentially constant voltage. Curve B shows the electrical response of the resistive layer-aluminum layer junction for the case of the gold dot electrically positive with respect to the aluminum. For aluminum positive with respect to the gold a similar result occurs; however, a lower value of the saturation voltage is observed. Hence, the bipolar voltagecurrent response is asymmetric around 0 V. The effect of driving current through the junction with aluminum positive is to switch the junction into a lower resistance state, with the reduction in resistance proportional to the current density. (The observation that junctions of this type can switch states was made earlier by Tsai [5] as part of an investigation of graphite-aluminum composites.) The singlecycle full bipolar voltage-current response of this junction region is thus highly hysteretic.

Scanning Auger electron microscopy depth profiles were taken through the aluminum film toward the resistive layer. Although the resultant spectra are difficult to interpret because of surface roughness effects, they seem to indicate the presence of an oxide region between the aluminum and resistive layer. Conduction through the interface is then likely to be barrier-dominated. It is hypothesized that this oxide barrier contains regions and/or channels of high

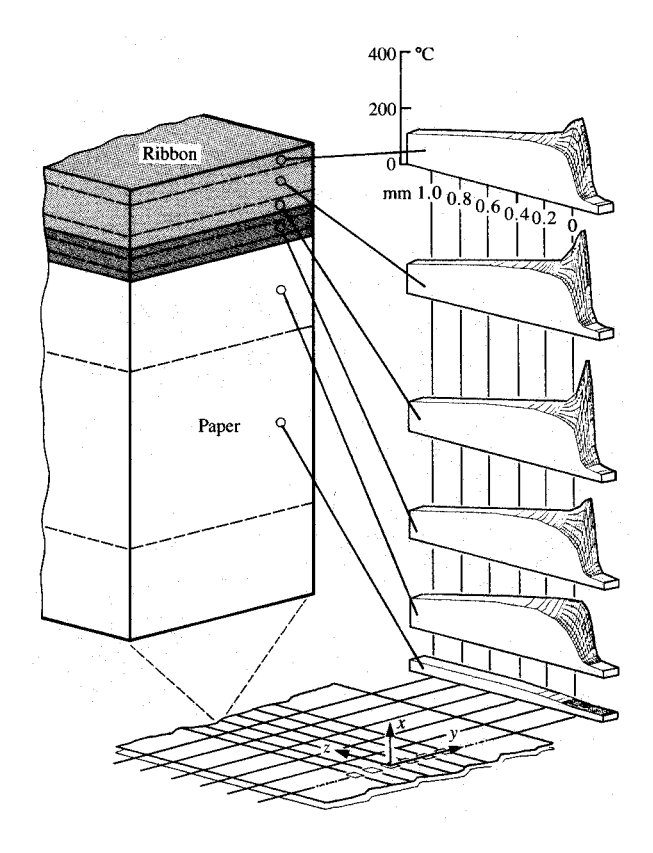


Electrode-aluminum voltages to maintain current pulses for (a) one energized electrode; (b) center of seven energized electrodes.

conductivity. Conduction through these regions and their enhancement or disruption due to material changes of state brought about by the persistent application of electric fields give rise to the shape of the bipolar voltage-versus-current response.

Curve C is for a test configuration in which a metal probe with a circular end face replaces the gold dot for current injection into the resistive layer-aluminum layer structure. As before, the voltage-current response of this arrangement can be determined by noting the voltage required to sustain a current ramp. At a given current density, the voltage level of curve C is greater than the sum of the corresponding voltages of curves A and B. This voltage difference presumably results from a contact resistance introduced by the probe into the current flow path. The total surface area of a probe loaded under pressure against the resistive layer does not participate in conduction; an increase in circuit resistance arises from current flow through small local-area contact spots (constriction resistance) and a specific contact resistivity (in units of  $\Omega$ -mm<sup>2</sup>) possibly caused by thin insulating films.

Curves A, B, and C of Fig. 4 were obtained from idealized configurations and provided information about the nature of the current flow path in the resistive ribbon thermal transfer printing process. **Figure 5** gives the voltages required to



Ribbon and paper region modeled in the numerical simulation with predicted temperature distributions which exist throughout this structure at the end of a 12.5-ms, 25-mA current pulse.

initiate and sustain constant current pulses in the electroderibbon structure. These voltages represent electrode-toaluminum values; the voltage drop along the ground path is not included. Data for a single electrode and for the center electrode of seven energized electrodes are plotted. All curves are the average of 20 measurements. The voltage level for a 5-mA current is roughly three times greater in the multipleelectrode case than in the single-electrode case. For a single electrode the current density through the compositealuminum interface is relatively low; the through voltage is primarily fixed by contact and composite resistances and the near-ohmic behavior of the resistive layer-aluminum junction. In the multiple-electrode case, current focusing caused by energizing the adjacent electrodes results in higher current densities through the ribbon structure and forces the resistive layer-aluminum interface into the nonlinear region. In this case the electrode-to-aluminum voltage includes a higher interface voltage offset as well as the contributions due to contact and composite resistances. For higher currents the single-electrode case remains linear until

approximately 12 mA. For one energized electrode, currents greater than or about equal to 12 mA are required to drive the composite–aluminum interface into the nonlinear state; at these current values a leading-edge voltage transient appears as in all multiple-electrode traces. The leading transient is believed to result from contact heating and from the resultant reduction of contact resistance as a more intimate electrode-to-resistive layer contact forms due to resistive layer softening.

A current level of approximately 25 mA is nominally required by the printing process. The corresponding input power per electrode is approximately 190 mW, or 0.002 J/mm lineal input energy at 102 mm/s electrode speed.

# Temperatures of the process

Any effort to measure process temperatures in the regions of the electrode contact area and the ribbon region beneath this contact area is complicated by the physical arrangement of these items. Estimates of the printing process temperatures have relied on numerical models and the comparison of these models with temperature measurements near the contact areas. In the work described in this section, the modeling was accomplished by application of the 5796-PBH Advanced Statistical Analysis Program (ASTAP) [6]. This program provides procedures for use in the design and reliability analysis of linear and nonlinear electrical networks. It can also be used to simulate any physical system that can be described by an analog electrical network. With this program, a time-dependent, three-dimensional, movingmaterial, coupled electrical-thermal model of the electroderibbon-paper structure was derived. Figure 6 illustrates the various components of the simulation region. In determining the region to be simulated, the electrical and thermal symmetry for an energized electrode near the center of the array was used to bound the region in the y direction between x-z planes passing through the center of electrodes and between electrodes. The extent of the modeled region in the negative z direction, that is, toward unused ribbon, is relatively short and reflects the low heat flow occurring in this direction. In the positive z direction, a relatively long distance is modeled to give temperature information in the region where transfer materials leave the ribbon and adhere to the paper in the printing process. The peeling action as the ribbon detaches from the paper is not modeled. In the vertical or x direction, the simulation space extends from the bottom surface of the paper to the top surface of the resistive layer or to a point in the electrode above the contact face. These extremes are assumed to be at ambient temperatures. The ribbon and paper within these boundaries are stratified into the seven layers shown in the figure; these layers are further divided into smaller volumes or cells by a set of orthogonal x-y and x-z planes. The relative positions of these planes are chosen to give the cells a small volume in the regions where large temperature gradients are expected and,

474

conversely, a large cell volume for regions with small temperature gradients.

Before ASTAP can be applied to a particular engineering problem, an analog electrical network must be constructed which closely resembles the physical attributes of the system to be simulated. In the model network used here, the electrode and contact resistances are modeled as single resistors, with the contact resistor connected between the electrode tip and the top cell in the resistive layer. The cells in the ribbon layers in the current flow path are each modeled as three-dimensional resistor networks. These resistors are assigned values determined from the temperature-dependent resistive properties of the layer materials and the dimensions of the cells. The resistive layer-aluminum layer interface is modeled so as to permit low current density flow through a constant interface resistance; at high current density the flow is at a fixed voltage through a low incremental resistance.

Passing current through the network produces heat within the physical cells containing the elements. This heat is coupled into the equivalent thermal simulation of the cells. The thermal network is represented through an interconnection of resistors, capacitors, and current sources in which the resistors represent thermal conductivities, the capacitors permit heat energy storage, and the current sources simulate energy flows due to internal power dissipation and transport effects. The energy dissipated in the contact resistance is coupled into the top quarter of the resistive layer under the electrode contact area. The resultant node voltages in the thermal lattice represent the temperature distribution through the modeled space.

In this model, a simulation region is specified for the assumption of an infinite array of energized electrodes. This assumption applies best during printing for an electrode near the center of many energized electrodes. For electrodes at the extremes of the array, or for isolated energized electrodes, heat can flow through the *x-z* plane boundary located at negative *y*. All electrode and ribbon temperatures in these instances are lower. The electrical and thermal properties of the materials were obtained from direct measurements or from the literature. The physical dimensions of the ribbon structure are held constant throughout the simulation. This approximation does not fully model transfer layer flow into the paper structure or the embossing action by the electrodes of the top surface of the resistive layer under high current flow conditions.

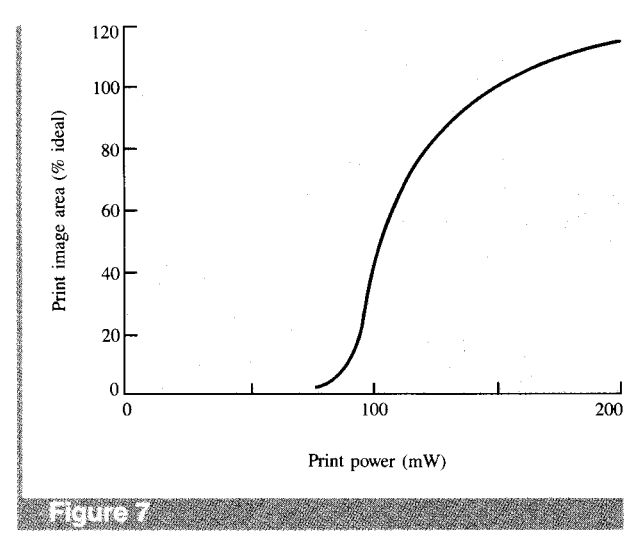
The temperatures (degrees Celsius) as predicted by the model are shown in Fig. 6 for a situation in which the electrodes slide over the ribbon at a rate of 102 mm/s. (The scales in these plotted distributions are chosen so that a given length along the y axis represents half the physical distance of an equal length in the z direction.) At time zero a current of 25 mA begins to flow in the ribbon structure; the flow is maintained for 12.5 ms, the time required for the

electrodes to traverse half the width of characters spaced at 10 to the inch. The temperature distributions shown are those predicted by the model which exist at at the end of the 12.5-ms current pulse.

In the negative z region, that is, upstream from the electrode array, the ribbon temperature is at an ambient value. As the point of observation moves toward the electrodes (the shaded areas on the distributions represent regions in the "shadow" of half an electrode), the temperatures rise sharply at the leading edge of the electrodes. Ribbon materials passing directly under the electrodes rise to much higher temperatures than materials between electrodes. The model indicates that the peak temperatures in the ribbon are attained in the region containing the composite-aluminum junction. This shows that the printing process creates intense heat directly at one surface of the transfer materials. As the ribbon streams from under the electrodes, the peak temperatures from the top of the resistive layer to the middle of the transfer layer fall rapidly, while temperatures in the track of the electrode at the transfer layer-paper interface rise until  $z \approx 0.1$  mm. Concurrently, the temperatures of materials between electrodes rise rapidly. At  $z \approx 0.2$  mm, the ribbon temperatures (downstream from the energized electrodes) reach a nearly constant value. For larger z, the ribbon temperature falls slowly.

The predicted electrode-tip peak temperature at the end of the 12.5-ms current pulse is less than the peak ribbon temperature at the top surface of the resistive layer as a result of a thermal contact resistance included in the model. The value of the thermal contact resistance was estimated from a combination of simulation studies and experimental measurements of current flow through small-diameter pressure probes loaded against a sheet of resistive layer.

The general shape of these temperature distributions holds for both shorter and longer simulation times, with the temperatures rising to somewhat higher values for longer periods of time. The longer simulation times more closely resemble the conditions for some laboratory temperature measurements and the model is in reasonable agreement with these measurements. For example, the temperature of a point on the top surface of the resistive layer, 0.7 mm downstream and centered on five energized electrodes, was measured to be approximately 250°C on an experimental arrangement of the process. The model predicts 242°C. On another prototype arrangement in which the paper layer was replaced by an infrared transmitting window, transfermaterial temperatures on the order of 300°C were measured under electrodes; much lower temperatures were observed between electrodes. Simulation results give peak temperatures of 277°C at the transfer layer-paper interface region. The model is in reasonable accord with experiment and explains the salient features of the printing process temperature distributions.



Area of the printed image versus power supplied per electrode during printing.

# **Printer response**

On the basis of the electrical and thermal description of the printing process, it is possible to propose the manner in which characters are formed. Figure 6 shows the predicted higher temperatures reached by the transfer materials passing under the electrodes relative to those of the transfer materials adjacent to these regions. This high temperature coupled with the high pressure exerted by the electrodes establishes a transfer layer-paper bond. As the ribbon passes from under the electrodes, the transfer materials in peripheral regions rise in temperature. The tensile strength of the transfer layer and the transfer layer-aluminum bond strength are reduced in the larger heated area. When the ribbon is directed away from the paper at the trailing edge of the printhead structure, the transfer layer-paper bond overcomes the transfer laver-aluminum bond, and the heated transfer material tears from the ribbon and adheres to the paper.

The size of the printed mark on the paper correlates well with the predicted average temperature of the ribbon layers downstream from the electrodes. In this experiment, print currents for nominal character areas were measured for ribbons with layers of various thicknesses. Then temperature distributions as a function of electrode current were obtained with the ASTAP simulation model for each ribbon in this parametric set. The average temperature at approximately 0.1 mm downstream from the trailing edges of the electrodes was computed. The temperature distributions with average temperatures equaling the average for the nominal case were noted. Finally, the print currents corresponding to this subset of distributions were compared to those in the printing portion of the study. The currents predicted by the model for establishing a constant average temperature at the

electrode trailing edge are within about 1.0 mA of the printing currents to maintain constant print area.

The ribbon temperature downstream from the electrodes is known from other work on development apparatus to vary with input power. Therefore, the input power should also relate to the area of the printed character. Through dimensional analysis, it can be shown that a normalized area should relate to the ratio of the lineal input energy to the energy per unit length required to raise the transfer layer material to some fixed temperature. This assertion was tested for the print characteristics of a number of different ribbon formulations and layer thicknesses, printhead-to-ribbon speeds, and electrode sizes. A strong correlation between the two dimensionless parameters was obtained over the relatively large energy ratios considered. For a particular process configuration, with the electrode size and speed fixed along with the ribbon structure and formulation, an equivalent relationship between normalized area and input power should also exist. A relationship of this type is shown in Figure 7. Input power in this figure is defined as the electrode-to-aluminum voltage times print current for an energized electrode. No transfer materials adhere to the paper for input powers per electrode less than approximately 70 mW. As the input power rises from slightly below to slightly above 100 mW, the percentage of area increases rapidly from 0 to 80. Beyond 150 mW, the character area changes more slowly with input power.

### Summary

This paper characterizes the resistive ribbon thermal transfer printing process. It provides a description of the voltage-versus-current response of the electrode-ribbon circuit, the temperature distributions throughout the ribbon, and the correlation between print response and electrical input and temperatures within the ribbon structure.

The electrode-ribbon circuit is discussed in terms of the elements of a simple lumped parameter model. In this model a temperature-dependent resistor represents the polycarbonate-carbon composite layer of the ribbon. Two other elements describe the composite-metal junctions in the circuit. The composite-aluminum junction has a highly nonlinear voltage-current response. At print conditions, this junction appears to pass large current densities at a fixed voltage. The composite-electrode junction is described in terms of a contact resistance. The electrical responses of the elements of this simple model help explain the voltage versus current response of the electrode-ribbon circuit. A nominal input power per electrode of approximately 190 mW is noted.

The simulation program provided an estimate of the temperature distribution throughout the ribbon structure. This predicted that the highest ribbon temperatures during printing occur in ribbon materials passing under the electrodes. The predicted hottest region in the ribbon

structure surrounds the composite-aluminum interface and creates intense heat at one surface of the transfer materials. Ribbon material temperatures between electrodes and on line with the electrode array are considerably lower. Once heated, the ribbon structure downstream from the energized electrodes reaches some constant temperature.

Finally, the area of the printed image is shown to correlate with the average ribbon temperature downstream from the electrodes and with the electrical input power.

# **Acknowledgments**

The work of N. C. Watkins in characterizing carbon-polycarbonate composites is recognized; B. M. Cassidy, D. S. Fields, and K. A. Meece have contributed greatly to the understanding of the current-voltage response of the process; R. M. Wooton's work in simulating the process through electrothermal models is significant; the temperature measurements resulted from the efforts of A. S. Campbell and those directed by D. B. Dove. R. D. Fathergill and F. V. Evridge provided expert technical support for much of this work.

## References

- D. A. Newman, "Planographic Printing," U.S. Patent 2,713,822, 1955.
- L. Montanari and F. Knirsch, "Electro-Thermic Printing Device," U.S. Patent 3,744,611, 1973.
- K. S. Pennington and W. Crooks, "Resistive Ribbon Thermal Transfer Printing (R2T2): A New Printing Technology," Technical Abstracts, Second International Congress on Non-Impact Printing, Society for Photo-Optical Scientists and Engineers, Springfield, VA, 1984, p. 236.
- R. D. Sherman, L. M. Middleman, and S. M. Jacobs, "Electron Transport Processes in Conductor-Filled Polymers," *Polymer Eng. & Sci.* 23, 36–46 (1983).
- S. Tsai, "The Characterization of the Interface in Graphite-Aluminum Composite Systems," Ph.D. Thesis, University of Texas, 1980.
- IBM Program Product No. 5796-PBH, Advanced Statistical Analysis Program (ASTAP), Program Reference Manual, Order No. SH20-1118-0, available through IBM branch offices.

Received October 8, 1984; revised May 7, 1985

**Thomas G. Twardeck** *IBM Information Products Division, 740 New Circle Road, Lexington, Kentucky 40511.* Dr. Twardeck is a senior engineer in new product development. Prior to joining IBM at Lexington in 1974, he was involved with plasma diagnostic techniques and submerged arc furnace design. At IBM he has worked on the development of printer products and test strategies for hardware and software. Dr. Twardeck received a Ph.D. in electrical engineering from Pennsylvania State University, University Park, in 1968.